THE JOURNAL OF PHYSICAL CHEMISTRY Letters

Letter

pubs.acs.org/JPCL

Correlated Rectification Transport in Ultranarrow Charged Nanocones

Wen Li,[†,#] Youguo Yan,[†,#] Muhan Wang,[†] Petr Král,[*,‡,§,∥] Caili Dai,[⊥] and Jun Zhang[*,†]

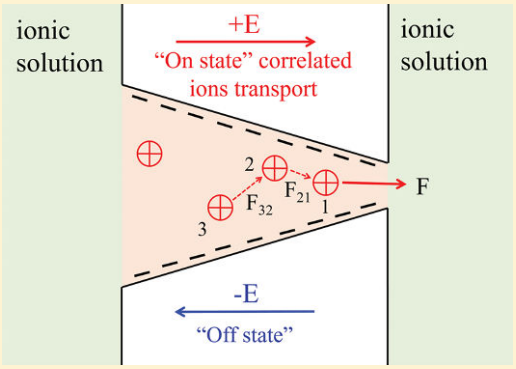
[†]College of Science, China University of Petroleum, Qingdao, Shandong 266580, People's Republic of China

[‡]Department of Chemistry, [§]Department of Physics, and [∥]Department of Biopharmaceutical Sciences, University of Illinois at Chicago, Chicago, Illinois 60607, United States

[⊥]State Key Laboratory of Heavy Oil Processing, China University of Petroleum, Qingdao, Shandong 266580, People's Republic of China

S *Supporting Information*

ABSTRACT: Using molecular dynamics simulations, we reveal ion rectification in charged nanocones with exit diameters of 1−2 nm. The simulations exhibit an opposite rectification current direction than experiments performed in conical channels with exit diameters larger than 5 nm. This can be understood by the fact that in ultranarrow charged cones screening ions are trapped close to the cone tip at both field directions, which necessitates them to be released from the cone in a correlated multi-ion fashion. Electroosmosis induced by a unidirectional ion flow is also observed.



Ion and molecular transport in synthetic nanochannels have widespread applications in nanofluidics, molecular separation, desalination, energy conversion, molecular sensing, and related fields.[1−4] Recently, ion current rectification was observed in asymmetric charged channels with diameters larger than 5 nm.[5−9] Although various nanofluidic channels have been built in 2D materials,[10,11] it is very challenging to prepare ultranarrow asymmetrical nanochannels allowing ion rectification.

In sub-2 nm channels, restricted screening, ion trapping, and dehydration can become very important.[12−14] As a result, various complex correlated ion transport regimes might take part in such ultranarrow channels, in analogy to those present in protein channels. It is of large interest to understand ion transport and rectification in such limiting synthetic systems. Because these systems are difficult to prepare and directly test experimentally,[15−17] one could try to understand their properties by modeling. Continuum theories have limited validity at the sub-nm scale. Instead, molecular dynamics (MD) simulations are often used to study ion transport behavior in nanochannels.[18−26] In this work, MD simulations are conducted to investigate ion transport in charged nanocone channels with exit diameters of 1−2 nm.

Figure 1 shows the studied system, which is composed of a fixed carbon nanocone (CNC) channel with an apex angle of 19.2° (length of L = 4.24 nm, exit diameters of D_1 = 0.89 nm and D_2 = 2.35 nm); narrow long cones provide better rectification. The cone is held between two fixed graphene sheets (3.936 × 3.835 nm^2), possessing holes matching the cone exits; the small (large) CNC exit is called a tip (base). The cone is homogeneously negatively charged with a total charge of Q = 0−15 e, the cone charge is neutralized by Na^+ counterions, a NaCl solution is placed outside of the graphene area (periodic boundary conditions), and the whole system is placed in an electric field of $|E|$ = 0−0.5 V/Å applied along the z axis. The homogeneously charged conical surface also generates a dipolar moment aligned along the z axis. However, due to a small apex angle and a cut tip, a dipolar field of the charged

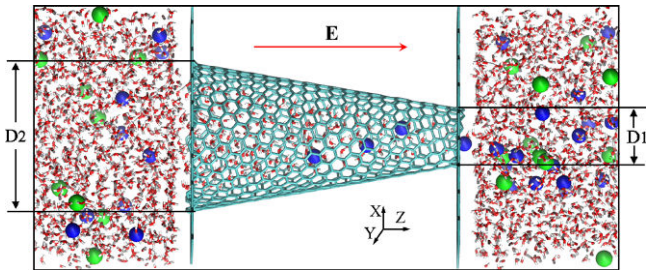


Figure 1. Simulation model. The negatively charged CNC is held between two graphene sheets with pores adjacent to the cone exits. The system is submerged in a NaCl solution, in the presence of driving electric fields. The blue/green balls denote Na^+/Cl^- ions.

Received: November 10, 2016
Accepted: December 30, 2016
Published: December 30, 2016

 © XXXX American Chemical Society

DOI: 10.1021/acs.jpclett.6b02640
J. Phys. Chem. Lett. 2017, 8, 435−439

cone presents a small contribution to the external field oriented in the same way.

The system was simulated with LAMMPS,[27] using the CHARMM force field[14] and the TIP3P water model.[28] The sp^2 carbon−carbon Lennard-Jones (LJ) parameters were σ_{CC} = 3.3997 Å and ε_{cC} = 0.0859 kcal/mol. Other LJ parameters were obtained from ref 29 and by using the Lorentz−Berthelot rules.[30] The van der Waals (vdW) coupling was calculated with a cutoff of 12 Å. All of the parameters are summarized in Table S1 (Supporting Information). The particle-particle-particle-mesh method was used to treat long-range electrostatic interactions. The simulations were conducted in an *NVT* ensemble at T = 298 K, with a 1 fs time step. A 20 ns simulation was conducted for each system, where the last 16 ns were used for data analysis.

Figure 2a shows current−voltage (I−V) characteristics for ions passing through CNC channels at different electric fields

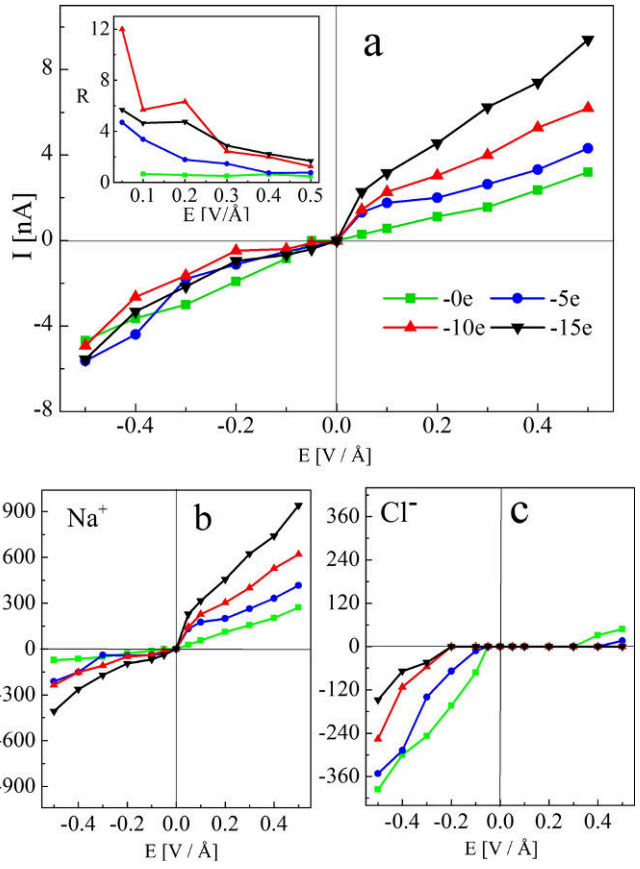


Figure 2. (a) I−V characteristics of a CNC channel with different surface charge densities. (inset) Corresponding rectification ratio. (b,c) Number of cations and anions passed through the systems in (a) within the same observation times (combination of results in (b,c) gives (a)). In (a−c), the green, blue, red, and black lines represent surface charges of 0, −5, −10, and −15 e, respectively.

and surface charge densities under a NaCl concentration of c = 0.427 mol/L. If the channel surface is not charged, the I−V curve is close to linear. When it is negatively charged, the system provides ion current rectification at small fields (different currents at opposite E fields). The inset shows a rectification ratio, $R = I_{+E}/I_{-E}$. We can see that R gradually decreases with increasing E. Moreover, the largest R is found for surface charges of Q = −10 e. The electric current, $I = (Q_a - Q_a)/t$, was calculated from the ratio of the total charge of cations (Q_c) minus that of anions (Q_a) passed through the cone and the time over which the ions have been passing through the channel.

To understand better the observed phenomena, we need to consider the symmetries of the studied systems associated with their charging. In principle, three charge configurations determine the system behavior: (1) ion charge (q), (2) cone charge (Q), and (3) external electric field direction (E). Therefore, we can characterize each situation by a "sign vector" (1,2,3) = (±,±,±). If we neglect slight differences between different ions (sizes, vdW) and the fact that water is not charge-symmetric, the situations with opposite charges behave in the same way. For example, the following pairs of cases have alike behavior: (+,+,+) and (−,−,−), (+,−,+) and (−,+,−), and (+,+,−) and (−,−,+). We will discuss the simulated results considering the above symmetries.

In Figure 2b,c, we resolve the ionic current into cationic (Na^+) and anionic (Cl^-) contributions. Interestingly, the conical nanochannel shows highly asymmetric passage rates for individual ions even at Q = 0. At around E = 0, the passage rates have to be symmetric due to thermodynamics principles. However, in nonlinear regimes, the passage rate is very different at ±E. The passage rate is larger when the ions approach the cone from the extended side due to a higher likelihood of collecting ions from the solution. This takes part for cations (anions) at E > 0 (E < 0), thus reflecting the above symmetries at Q = 0. The reasons why the I−V curve (at Q = 0) for cations is not identical to that for anions (upon flipping E and I), as seen in Figure 2b,c, are the nonlinear nature of the water dipole and the fact that the ions have different radii.

At $Q \neq 0$, the above symmetries are lost because only one of the two ions is preferentially attracted to the cone. At relatively small Q, both cations and anions can still pass the channel, but their passage rates become already quite different, especially at $|E| < 0.3$ V/Å. When Q grows, the favored ions are more attracted to the channel and can pass through it, while the disfavored ions almost cannot pass through it ($|E| < 0.3$ V/Å), as seen in Figure 2b,c. Ultimately, either cations or anions contribute to transport, while disfavored ions are blocked from it. At these high Q, ions develop a complex mechanism of cone passage, where they need to be first released from traps by other ions before being able to pass (see later) . Thus, the inherent asymmetry of I−V characteristics for individual ions (here Na^+) is behind the origin of the total ion rectification presented in Figure 2a. The discussed system has an approximate symmetry only when all three parameters (q, Q, E) are flipped over.

Rectification experiments performed in negatively charged cones with larger tips (D > 5 nm) show that ions preferentially pass the cones from the tip side,[5−9,13,31−33] in contrast to the current systems. In these experimental systems performed in larger cones, a profound electrostatic ratchet model was proposed to rationalize the current rectification direction.[6,34,35] In this model, there exists a Coulombic trap near the tip when cations transport from the base to the tip side (Figure 3a under +E) and suppress ion transport. However, the Coulombic trap will disappear when the cations transport from the tip to the base side under −E. Therefore, it is favorable for cations to transport from the tip to the base side. In general, ratchets are characterized by the presence of channel asymmetry and nonequilibrium conditions.

DOI: 10.1021/acs.jpclett.6b02640
J. Phys. Chem. Lett. 2017, 8, 435−439

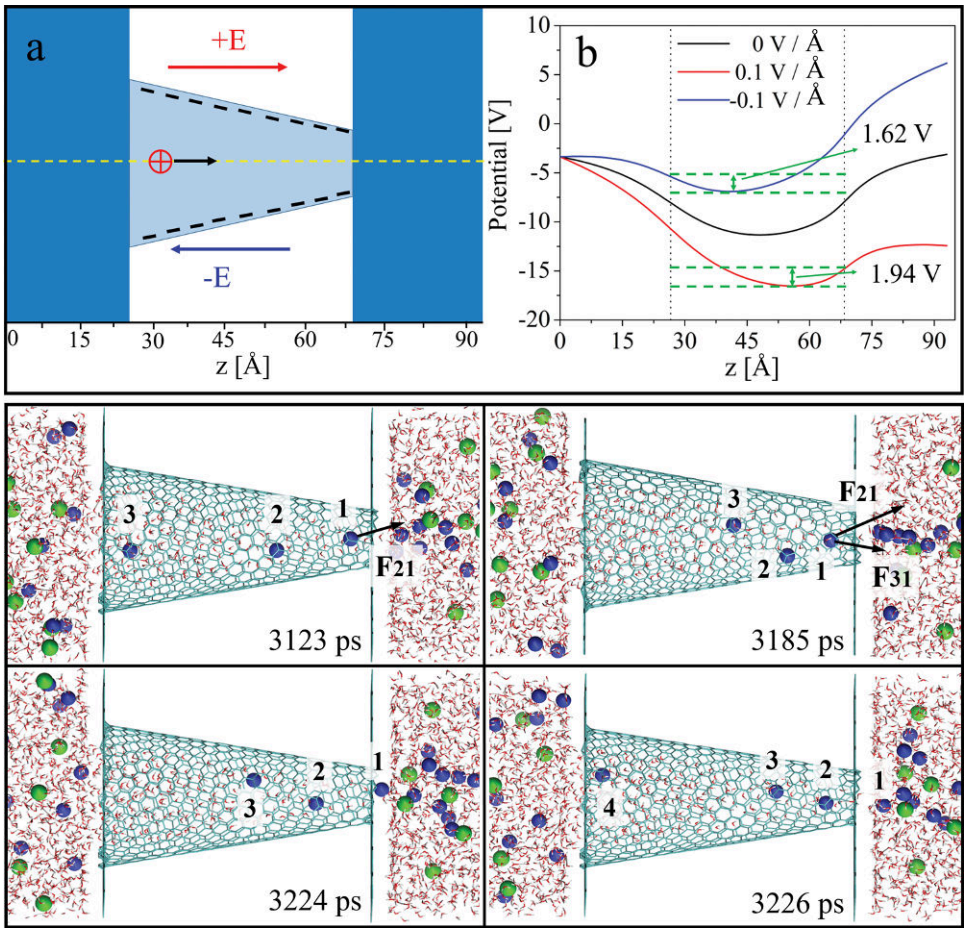


Figure 3. (top) Schematic of Coulombic ion trapping. (a) Model of a negatively charged conical nanochannel with a passing cation; (b) distributions of the intrinsic electrostatic potential and the potential as $\pm E$ applied along the axis of our ultranarrow nanocone channel. The regions between the dashed lines in (b) represent the conical channel region. (bottom) Snapshots of ion transport controlled by ion dehydration accompanied by correlated ion passage ($Q = -10$ e, $E = \pm 0.1$ V/Å).

In ultranarrow charged cones, the ions transport is different. In Figure 3b, the potential profile is calculated through the electrostatic potential integration of the channel surface charges, in the presence of $\pm E$ fields. It shows that the Coulombic trap exists in both field directions. Therefore, the passing ion needs to be first released from the trap, which can be done by other ions. However, to exert enough force, those ions must come from the wider channel region, which explains the opposite rectification current. Figure 3 (bottom) illustrates this correlated sequential passage of ions, where the ion (1) closest to the tip is initially trapped and then released from the trap and removed from the cone.

Our simulations show that the ions passing through the ultranarrow tip also need to be partly dehydrated. We can see this from a simple estimate. The effective transport radius of these channels equals their spatial radius, $D/2$, minus the vdW radius of carbon (wall) atoms ($r_C = 0.17$ nm),[36] giving $r_{tip} = 0.275$ nm and $r_{base} = 1.005$ nm for the two cone exits. The naked and hydrated radii of Na^+ are 0.116 and 0.358 nm, respectively.[37] Thus, Na^+ must be also partially dehydrated prior to passing through the ultranarrow tip. The correlated ion passage (rectification) described above is predominant at low electric fields and high surface charge densities, which corresponds to a high rectification ratio R, as shown in Figure 2a (see Table S2 and the Supporting Information movie) .

In general, electrostatic screening can play an important role in ion transport through confined nanochannels. We can briefly explore screening effects in the currently modeled systems by simulating them at different NaCl molar concentrations of $c = 0.821$, 0.427, and 0.048 mol/L, giving Debye lengths of $\lambda_D = 0.334$, 0.463, and 1.375 nm, respectively. Consequently, $r_{small} < \lambda_D < r_{large}$ at $c = 0.821$ and 0.427 mol/L, but r_{small}, $r_{large} < \lambda_D$ at $c = 0.048$ mol/L. Simulations presented in Figure 4 demonstrate that at low ionic strengths the passing currents are small. This is caused by the lack of screening, which makes it hard for the trapped ions to be released and pushed through the tip in a correlated manner.

Given the asymmetric flow of ions observed in these charged and electrified nanochannels, one could also expect them to manifest electroosmosis.[38,39] Figure 5 shows drag of water by the passing ions in systems presented in Figure 2a. From the large similarity of the curves on both figures, one can see a strong correlation between the passing ions and water. One can assume that every passing ion manages to pass part of its hydration shell and other waters around it (in narrow channels).[39] The inset shows the number of passing Na^+ ions and water molecules as a function of time through a typical channel with $Q = -10$ e and at $E = 0.1$ V/Å. The ratio of passing waters and Na^+ ions is $R_w \approx 8$, which is almost twice more than the number of hydrated water molecules around each Na^+.

DOI: 10.1021/acs.jpclett.6b02640
J. Phys. Chem. Lett. 2017, 8, 435−439

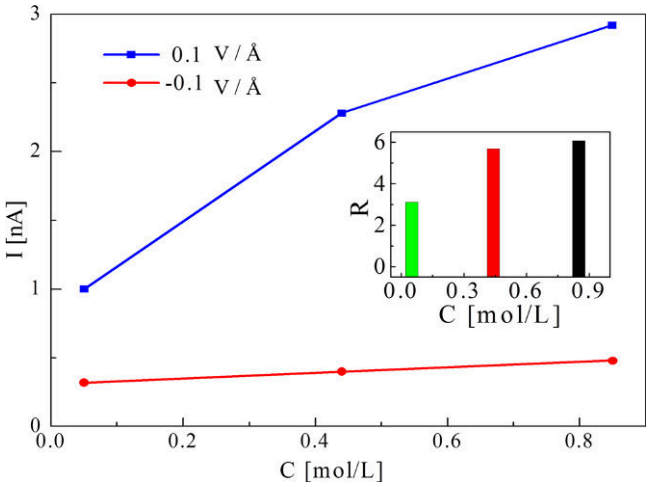


Figure 4. Ion current in a CNC channel with a surface charge of $Q = -10$ e at an electric field intensity of $E = \pm 0.1$ V/Å. (inset) The rectification ratio, R, at salt concentrations of $c = 0.05$, 0.44, and 0.85 mol/L.

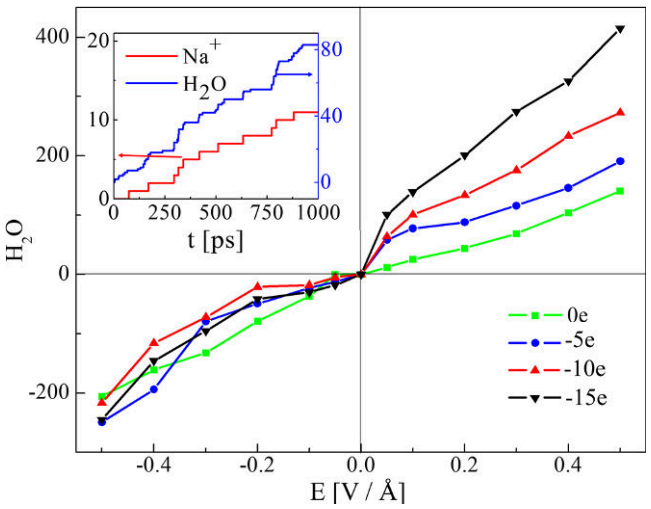


Figure 5. Electroosmosis in CNCs at surface charge densities as in Figure 2a. (inset) Time-dependent number of passing water molecules and Na^+ ions in a CNC with $Q = -10$ e at $E = 0.05$ V/Å.

In summary, using classical MD simulations, we have observed ion rectification in charged conical nanochannels with exit diameters of 1−2 nm. The rectification current direction is opposite compared to that reported in experiments performed in conical channels with exit diameters larger than 5 nm. This can be understood by the fact that in ultranarrow (1−2 nm) charged cones ions need to be first released from traps and partially dehydrated before being able to leave the cone. This correlated ion transport mode proceeds from the base to the tip side of the cone and results in the opposite rectification direction. Electroosmosis induced by unidirectional ion flow was also observed. These correlated rectification transport phenomena present in ultranarrow synthetic nanochannels can trigger further studies of functionalized nanofluidic devices. They might also shed light on ion transport in biological ion channels.

■ ASSOCIATED CONTENT

Supporting Information

The Supporting Information is available free of charge on the ACS Publications website at DOI: 10.1021/acs.jpclett.6b02640.

LJ and charge parameters and a list of the correlated ion passage mode (PDF)

Movie showing correlated ion passage (MPG)

■ AUTHOR INFORMATION

Corresponding Authors

*E-mail: pkral@uic.edu (P.K.).

*E-mail: zhangjun.upc@gmail.com (J.Z.).

ORCID

Petr Král: 0000-0003-2992-9027

Author Contributions

#W.L. and Y.Y. contributed equally.

Notes

The authors declare no competing financial interest.

■ ACKNOWLEDGMENTS

This work was funded by the National Basic Research Program of China (2014CB239204, 2015CB250904), the National Natural Science Foundation of China (U1262202, 51302321), the Shandong Provincial Natural Science Foundation, China (ZR2014EEM035), and the Fundamental Research Funds for the Central Universities (15CX08003A, 14CX05022A, 15CX05049A, 15CX06073A).

■ REFERENCES

(1) Hille, B. *Ion Channels of Excitable Membranes*; Sinauer Associates, Incorporated: Sunderland, U.K., 2001.

(2) Li, W.; Bell, N. A.; Hernández-Ainsa, S.; Thacker, V. V.; Thackray, A. M.; Bujdoso, R.; Keyser, U. F. Single Protein Molecule Detection by Glass Nanopores. *ACS Nano* **2013**, *7*, 4129−4134.

(3) Duan, R.; Xia, F.; Jiang, L. Constructing Tunable Nanopores and their Application in Drug Delivery. *ACS Nano* **2013**, *7*, 8344−8349.

(4) Duan, C.; Majumdar, A. Anomalous Ion transport in 2−*nm* Hydrophilic Nanochannels. *Nat. Nanotechnol.* **2010**, *5*, 848−852.

(5) Gamble, T.; Decker, K.; Plett, T. S.; Pevarnik, M.; Pietschmann, J. F.; Vlassiouk, I.; Aksimentiev, A.; Siwy, Z. S. Rectification of Ion Currentin Nanopores Depends on the Type of Monovalent Cations: Experiments and Modeling. *J. Phys. Chem. C* **2014**, *118*, 9809−9819.

(6) Siwy, Z.; Heins, E.; Harrell, C. C.; Kohli, P.; Martin, C. R. Conical-nanotube Ion-Current Rectifiers: The Role of Surface Charge. *J. Am. Chem. Soc.* **2004**, *126*, 10850−10851.

(7) Pevarnik, M.; Healy, K.; Davenport, M.; Yen, J.; Siwy, Z. S. A Hydrophobic Entrance Enhances Ion Current Rectification and Induces Dewettingin Asymmetric Nanopores. *Analyst* **2012**, *137*, 2944−2950.

(8) Vlassiouk, I.; Siwy, Z. S. Nanofluidic Diode. *Nano Lett.* **2007**, *7*, 552−556.

(9) Guo, W.; Tian, Y.; Jiang, L. Asymmetric Ion Transport through Ion-Channel-Mimetic Solid-State Nanopores. *Acc. Chem. Res.* **2013**, *46*, 2834−2846.

(10) Koltonow, A. R.; Huang, J. Two-Dimensional nanofluidic. *Science* **2016**, *351*, 1395−1396.

(11) Yang, X.; Cheng, C.; Wang, Y.; Qiu, L.; Li, D. Liquid-Mediated Dense Integration of Graphene Materials for Compact Capactive Energy Storage. *Science* **2013**, *341*, 534−537.

(12) Israelachvili, J. N. *Intermolecular and Surface Forces*; Academic Press: London, U.K, 1991.

(13) Siwy, Z. S. Ion-Current Rectification in Nanopores and Nanochannels with Broken Symmetry. *Adv. Funct. Mater.* **2006**, *16*, 735−746.

(14) Cohen-Tanugi, D.; Grossman, J. C. Water Desalination Across Nanoporous Graphene. *Nano Lett.* **2012**, *12*, 3602−3608.
(15) Liu, H.; He, J.; Tang, J.; Liu, H.; Pang, P.; Cao, D.; Krstic, P.; Joseph, S.; Lindsay, S.; Nuckolls, C. Translocation of Single-Stranded DNA through Single-Walled Carbon Nanotube. *Science* **2010**, *327*, 64−67.
(16) Holt, J. K.; Park, H. G.; Wang, Y.; Stadermann, M.; Artyukhin, A. B.; Grigoropoulos, C. P.; Noy, A.; Bakajin, O. Fast Mass Transport through Sub-2-Nanometer Carbon Nanotube. *Science* **2006**, *312*, 1034−1037.
(17) Rhee, M.; Burns, M. A. Nanopore Sequencing Technology: Nanopore Preparation. *Trends Biotechnol.* **2007**, *25*, 174−181.
(18) Hummer, G.; Rasaiah, J. C.; Noworyta, J. P. Water Conduction through the Hydrophobic Channel of a Carbon Nanotube. *Nature* **2001**, *414*, 188−190.
(19) Hummer, G. Water, Proton, and Ion Transport: From Nanotubes to Proteins. *Mol. Phys.* **2007**, *105*, 201−207.
(20) Berezhkovskii, A.; Hummer, G. Single-File Transport of Water Molecules through a Carbon Nanotube. *Phys. Rev. Lett.* **2002**, *89*, 064503.
(21) Kalra, A.; Garde, S.; Hummer, G. Osmotic Water Transport through Carbon Nanotube Membranes. *Proc. Natl. Acad. Sci. U. S. A.* **2003**, *100*, 10175−10180.
(22) Goh, P. S.; Ismail, A. F.; Ng, B. C. Carbon Nanotubes for Desalination: Performance Evaluation and Current Hurdles. *Desalination* **2013**, *308*, 2−14.
(23) Goldsmith, J.; Martens, C. C. Molecular Dynamics Simulations of Salt Rejection in Model Surface-Modified Nanopores. *J. Phys. Chem. Lett.* **2010**, *1*, 528−535.
(24) Corry, B. Water and Ion Transport through Functionalised Carbon Nanotubes: Implications for Desalination Technology. *Energy Environ. Sci.* **2011**, *4*, 751−759.
(25) Zhao, K.; Wu, H. Fast Water Thermo-Pumping Flow Across Nanotube Membranes for Desalination. *Nano Lett.* **2015**, *15*, 3664−3668.
(26) Gong, X.; Li, J.; Xu, K.; Wang, J.; Yang, H. A Controllable Molecular Sieve for Na^+ and K^+ Ions. *J. Am. Chem. Soc.* **2010**, *132*, 1873−1877.
(27) Plimpton, S. Fast Parallel Algorithms for Short-Range Molecular Dynamics. *J. Comput. Phys.* **1995**, *117*, 1−19.
(28) Jorgensen, W. L.; Chandrasekhar, J.; Madura, J. D.; Impey, R. W.; Klein, M. L. Comparison of Simple Potential Functions for Simulating Liquid Water. *J. Chem. Phys.* **1983**, *79*, 926−935.
(29) Joung, I. S.; Cheatham, T. E., III Determination of Alkali and Halide Monovalent Ion Parameters for Use in Explicitly Solvated Biomolecular Simulations. *J. Phys. Chem. B* **2008**, *112*, 9020−9041.
(30) Werder, T.; Walther, J.; Jaffe, R.; Halicioglu, T.; Koumoutsakos, P. On the Water-Carbon Interaction for Use in Molecular Dynamics Simulations of Graphite and Carbon Nanotubes. *J. Phys. Chem. B* **2003**, *107*, 1345−1352.
(31) Harrell, C. C.; Kohli, P.; Siwy, Z.; Martin, C. R. DNA-Nanotube Artificial Ion Channels. *J. Am. Chem. Soc.* **2004**, *126*, 15646−15647.
(32) Cervera, J.; Schiedt, B.; Ramirez, P. A Poisson/Nernst-Planck Model for Ionic Transport through Synthetic Conical Nanopores. *Europhys. Lett.* **2005**, *71*, 35−41.
(33) Cheng, L. J.; Guo, L. Nanofluidic Diodes. *Chem. Soc. Rev.* **2010**, *39*, 923−938.
(34) Astumian, R. D. Making Molecules into Motors. *Sci. Am.* **2001**, *285*, 56−64.
(35) Nishizawa, M.; Menon, V. P.; Martin, C. R. Metal Nanotubule Membranes with Electrochemically Switchable Ion-Transport Selectivity. *Science* **1995**, *268*, 700−702.
(36) Bondi, A. van der Waals Volumes and Radii. *J. Phys. Chem.* **1964**, *68*, 441−451.
(37) Nightingale, E., Jr Phenomenological Theory of Ion Solvation: Effective Radii of Hydrated Ions. *J. Phys. Chem.* **1959**, *63*, 1381−1387.
(38) Král, P.; Wang, B. Material Drag Phenomena in Nanotubes. *Chem. Rev.* **2013**, *113*, 3372−3390.
(39) Vuković, L.; Vokac, E.; Král, P. Molecular Friction-Induced Electroosmotic Phenomena in Thin Neutral Nanotubes. *J. Phys. Chem. Lett.* **2014**, *5*, 2131−2137.

DOI: 10.1021/acs.jpclett.6b02640
J. Phys. Chem. Lett. 2017, 8, 435−439